Vazquez-Roy, J. L., Tamayo-Dominguez, A., Rajo-Iglesias, E., & Sierra-Castaner, M. (2019). Radial Line Slot Antenna Design With Groove Gap Waveguide Feed for Monopulse Radar Systems. *In IEEE Transactions on Antennas and Propagation, 67*(10), 6317–6324

DOI:10.1109/tap.2019.2922742

Radial Line Slot Antenna Design with Groove Gap Waveguide Feed for Monopulse Radar Systems

Jose Luis Vazquez-Roy, *Member IEEE*, Adrián Tamayo-Domínguez *Student Member IEEE*, Eva Rajo-Iglesias, *Senior Member, IEEE*, Manuel Sierra-Castañer, *Senior Member IEEE*.

***Abstract*—Radial Line Slot Arrays (RLSA) are well suited to be used in monopulse radar systems. The excitation of the sum and difference patterns can be achieved by the design of simple feeds as it is shown in this paper. A feed system based on the use of a cavity made in groove gap waveguide technology is presented in this work. The design is made at 24 GHz but can be easily scaled to higher frequencies as the technology is contactless and fully made in metal. A good isolation between the sum and difference ports together with a good matching of the two of them is obtained. The radiation patterns of the manufactured antenna are also in good agreement with the simulated ones.**

***Index Terms*—Radial Slot Array, Monopulse, groove gap-waveguide**

I. Introduction

Monopulse direction finding technique is a key function in modern surveillance and tracking radar systems. The monopulse operation can be achieved in different ways [1], [2]. In the amplitude comparison scheme, the signal received by a sum pattern antenna (Σ) is compared to the signals received by two difference pattern antennas in the azimuth and elevation planes ($\Delta_\phi, \Delta_\theta$) to extract the direction of arrival of the wavefront. In a different setup, a directive beam and a conical beam, both with rotationally symmetric amplitude distributions can be used. In this case, the conical beam has a radiation null on the broadside axis and a phase variation with azimuth. Then the direction of arrival can be extracted by a comparison between the amplitude of the received signals to extract the elevation angle, and a phase comparison to extract the azimuth angle, given that there is not any phase variation for the sum pattern with azimuth. The antenna presented in this manuscript uses this approach. We will keep the notation (Σ, Δ) to name the mentioned directive and conical beams hereafter.

Radial Line Slot Antennas (RLSA) are high gain planar antennas based on the excitation of cylindrical waves inside parallel-plate waveguides (PPWG) also known as radial lines, in which slots are introduced in the upper metalization of a two-sided metalized low loss dielectric. They are often used as antennas for monopulse radar application due to their high efficiency and ease of fabrication for microwave and millimeter wave frequency range. These antennas have very low transmission losses in the waveguide when compared with other lines such as microstrip or striplines.

The first concept of an RLSA was proposed by [3] in the 50s and demonstrated in the 60s by [4] but it was in the 80s when Ando et al. showed all the potential of this kind of antennas in [5]–[7]. These first examples were used for satellite reception at Ku band. In principle, these antennas are very attractive for high gain, circular polarization and moderate frequency band, as it was the case. For that purpose, a pencil beam was generated through a coaxial feed at the center of the antenna and with a spiral arrangement of the slots. If the slots are arranged in concentric rings, instead of a pencil beam, a conical or difference pattern is generated [8], [9] assuming again an excitation from the center of the PPWG with a coaxial feed. A sum pattern can also be obtained using concentric rings arrangement of the slots, if a phase rotating mode is generated inside the PPWG. This can be achieved in different ways as it was shown in [10], [11]. Other types of radiation patterns as well as a total control on the pattern characteristics can be also synthesized with this type of antennas (RLSA) as demonstrated in [12].

The monopulse application requires the simultaneous excitation of both patterns. This can be obtained by using two field distributions inside the parallel plate structure combined with concentric rings of slots. The two field distributions are implemented with two different input ports to provide the Σ and Δ patterns to implement the monopulse function as explained.

An example of the combination of these two modes to get a monopulse RLSA working at 14 GHz was presented in [13]. In that case, the feeding network includes a microstrip Butler matrix, but the losses were relatively high and consequently the idea cannot be scaled up in frequency.

Other examples of more complex implementations can be found in the literature in which the excitation of the radially symmetric modes is achieved by means of coupling slots between feeding waveguides [14] or coaxial cavities [10].

Recently, two papers describing monopulse antennas based in different gap-waveguide based structures have been published [15], [16]. This shows how the use of this technology facilities and simplifies the implementation of the monopulse function required in some communication and radar systems at microwaves and millimeter-wave bands. It is also clear that compactness of the feeding network is still an open issue.

Manuscript received May 23, 2019.

This work has been partly funded by the Spanish Government through projects TEC2016-79700-C2-2-R and TEC2014-55735-C3-1-R and by Madrid Regional Government under the project S2013/ICE-3000.

J.L. Vazquez-Roy and E. Rajo-Iglesias are with the Department of Communications and Signal Theory, Universidad Carlos III de Madrid, 28911 Madrid, Spain (e-mail: jvazquez, eva@tsc.uc3m.es).

A. Tamayo-Domínguez and M. Sierra-Castañer are with Department of Signals, Systems, and Radiocommunications, Universidad Politécnica de Madrid, 28040 Madrid, Spain (e-mail: a.tamayo, manuel.sierra@upm.es).

In this work, a Radial Line Slot Antenna with left-hand circular polarization is designed at 24 GHz to get the required amplitude and phase performance to be used in a monopulse radar. The antenna concept is the same explained in [13]. However, this paper introduces an optimization algorithm to design the radiating structure and a new feeding structure more compact and almost lossless to get the excitation of both antenna patterns. The fundamentals of the antenna optimization were presented in [17] whereas in [18], the preliminary design of the feeding network was introduced. This work proposes a new way to excite an RLSA antenna to achieve the mentioned Σ and Δ simultaneous patterns for monopulse operation by using a rectangular cavity excited by two coaxial probes (Σ and Δ channels) coupled to the radial line through a circular slot in the cavity lid that conforms a short section of coaxial waveguide when combined with the central probe, Σ. This cavity is implemented using groove gap waveguide technology [19]. This technology has been chosen because of the flexibility it introduces in the design, the ease of construction and its associated low ohmic losses [20], [21]. The proposed solution is simpler than other possible implementations although it provides narrowband operation.

The paper is divided in the following sections: Section II describes the antenna design, including the optimization process for the lengths and positions of the slots, Section III presents the design and the simulation results of the GWG cavity feed that will generate the field distributions that will be coupled to the RLSA to obtain the monopulse radiation patterns and, finally, Section IV contains the experimental results and some conclusions are drawn in Section V.

II. Antenna Design

In an RLSA antenna, the radiating element for circular polarization is basically a pair of orthogonal slots (seen in Fig. 1 for left-handed case) with a length close to resonance. If the slots are separated a quarter wavelength and they are orthogonal to each other, the polarization is circular. The relative position of one slot with respect to the other defines if the polarization is right or left handed. Also, due to the quarter wavelength separation between both slots, the reflection from one slot is almost canceled with the reflection from the second slot and the global reflection coefficient at the central frequency becomes low enough.

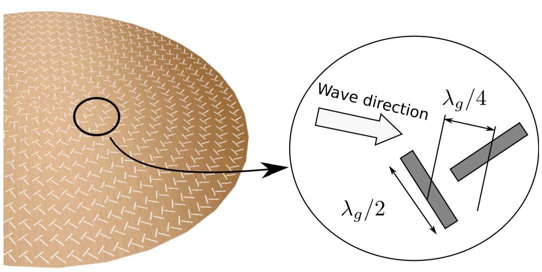

Fig. 1. Circular arrangements of slots for left handed circular polarization.

Assuming that the slots are arranged in concentric rings, the radiation pattern created by a TEM mode excited in the PPWG from the central point is a conical pattern, with a null in the broadside direction, i.e., a difference pattern. To generate the sum pattern with slots arranged in concentric rings, it is necessary to excite a phase rotating mode inside the parallel plate waveguide. This rotating mode must have constant amplitude and a linear phase with azimuth. The rotating mode can be generated in different ways. The simplest one is by using 4 coaxial probes excited with a phase difference of 90° between each consecutive feed. This is the method that was employed in [13] and the one used for the optimization of the slots arrangement in the current antenna design. Later on, in Section III this rotating mode will be generated with the new designed feed circuit.

For this design, a 20 cm diameter antenna, printed in PTFE material (ϵ_r=2.1, $\tan\delta = 2\cdot 10^{-4}$) is designed. The antenna, working at 24 GHz, has 9 rings of slots. Next section describes the process of optimization of the slots in the structure. The height of the parallel plate structure is 3.175 mm.

A. *Optimization of the radiating structure*

The synthesis of the slots can be performed using different methods. In our design, the optimization methodology is based on the algorithm presented in [22]. In this case, a hybrid algorithm based on two Matlab© functions (*simulated annealing* and *fmincom*) is used. The hybrid algorithm is used to make the process in two steps. First, a good solution using the global algorithm is found, and then, this solution is optimized searching for a local minimun. The optimization parameter is the antenna directivity. This is a compromise between amplitude and phase uniformity, and spillover efficiency (considering the residual power after the last ring of slots). This function presents multiple local minima and this is the reason for the use of a hybrid algorithm, combination of a global and a local algorithms. The error function to optimize is the difference between the directivity and the spillover efficiency for the sum pattern. The directivity is used in order to maximize the gain, since the effect of the losses is very small in this kind of antennas, as it can be seen in [23], [24]. It is necessary to include the spillover efficiency (residual power at the edge of the RLSA) since otherwise the algorithm can converge to very short non-resonant slots. These parameters are calculated with the software presented in [25], based on a single base function method of moments, very fast and accurate enough for the calculation of these parameters.

As mentioned, for the optimization of the position and length of the slots, the feeding network consists of a 4-pin structure with a phase difference of 90° between consecutive pins. This is done in order to be able to use the previous analysis tool, and in that way to make independent the design of the radiating structure with respect to the feeding network. With this assumption the results are accurate enough, and in a different way, it would be difficult to afford the optimization process. The output of the algorithm is the length for all the slots of each ring (identical for all the slots in one ring) and the central radial position for each ring of slots. Fig. 2 shows the results of the optimization process. As it can be observed, the slot length is increasing with the position of the ring in order to get uniform amplitude for the sum pattern. The slots are non-resonant, with a length slightly under resonance. The step between two consecutive rings is also a bit smaller than the wavelength in the waveguide. This is due to the effect of the slots in the phase of the propagating wave in the radial line. These two aspects are well explained in the references [5] to [13]. In a general case for long antennas, the distance between rings is typically around 0.95 times the wavelength in the dielectric.

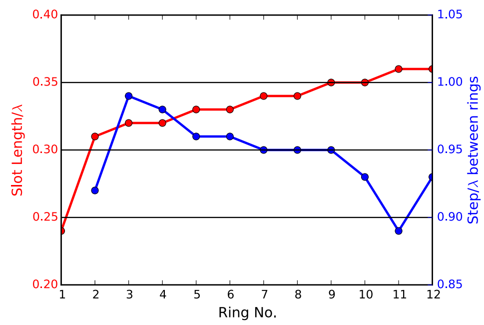

Fig. 2. Results of the optimization process for the slot lengths and the rings separation.

Fig. 3 shows the resulting radiation pattern for sum and difference excitations in one of the main planes (ϕ=0°). The predicted results are good enough for the application. In both patterns a good cross-polar radiation is obtained (below -25 dB) and the side lobe level is close to that of a uniform excitation.

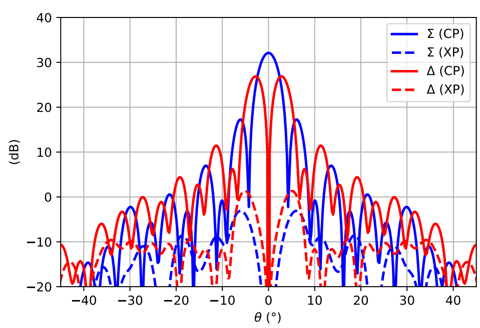

Fig. 3. Optimized sum and difference simulated radiation patterns (Gain) at 24 GHz for $\phi = 0°$ using MoM.

III. Feeding network design

The proposed design is based on the use of just two probes to excite all the required fields. One of them will directly excite the difference pattern whilst the spiral phase distribution will be obtained by using a degenerated cavity. As starting point, the excitation of only a parallel plate waveguide formed by the PTFE substrate with its two metalizations but without the radiating slots that later conform the RLSA antenna is considered. As mentioned before, the operation frequency is 24 GHz.

As a first step, a rectangular square-shaped waveguide cavity delimited by solid PEC walls was designed. Basically, the idea is to create two field distributions from three modes whose resonance frequencies must be close to the chosen 24 GHz operating frequency. These fields will later be coupled to the parallel plate structure that is above the structure by means of a circular slot located in the center of the cavity. With these three modes, two field distributions will be excited in the cavity: a rotating field composed by two 90° rotated similar modes excited in phase quadrature and a rotationally symmetrical mode having a maximum in the center of the cavity.

These two field distributions will be generated by means of two coaxial probes whose depth of penetration into the cavity must be adjusted as it is described in Fig. 4. In order to provide sufficient space to be able to introduce the excitation mechanism into the cavity, the following higher order cavity modes were chosen: $TE_{140}+TE_{410}|_{\pi/2}$ for the phase rotating field and TE_{330} for the symmetric one. The design of this initial cavity was made considering the excitation with four probes.

As a second step, a perturbation was introduced into the cavity with the aim of exciting the two needed field distributions with single coaxial probes, i.e., replacing the four probes by just two. Thanks to this perturbation, which does not affect very much to the to the initial symmetric mode distributions, it is possible to excite in phase quadrature the fields responsible for the phase rotating mode. In addition to this, the cavity was slightly modified, making it rectangular to compensate for the asymmetry introduced by the perturbation (seen in Fig. 4).

Regarding the coupling between the cavity and the PPWG above, a circular slot is made in the ground plane. This slot, together with the central excitation probe, conforms a short section of a coaxial waveguide that connects both elements. In essence, the symmetric field in the cavity will be coupled by means of the coaxial TEM mode, and the rotational cavity field, by rotating the coaxial TE_{11} mode. The slot radius will control the cutoff frequency and the propagating characteristics for the latter. This parameter and the ground plane thickness will be used to adjust the degree of coupling of these both fields to the PPWG.

As a final step, the vertical solid walls of the cavity were replaced by periodic squared pins to implement the aforementioned cavity using groove gap waveguide technology [19], to take advantage of the fact that that technology does not need electrical contact when assembling it with the antenna layer. Fig. 4 shows the final topology of the feed and how it is coupled to the PPWG.

For the final design, an optimization process was carried out using the full wave commercial software CST Microwave Studio©. Basically, the position and size (an inset in one of the cavity walls as it can be seen in Fig. 5), the penetration of the coaxial probes into the cavity, and the radius of the coupling circular slot were modified to improve the response in terms of phase and amplitude characterization of the generated fields in the PPWG and also in the full S-parameters response (good matching in the two ports together with a good isolation between them). It should be noted that the simulations demonstrated that a dense pin network to implement gap waveguide concept was needed to correctly adjust the position of the perturbation within the regular periodic lattice, thus

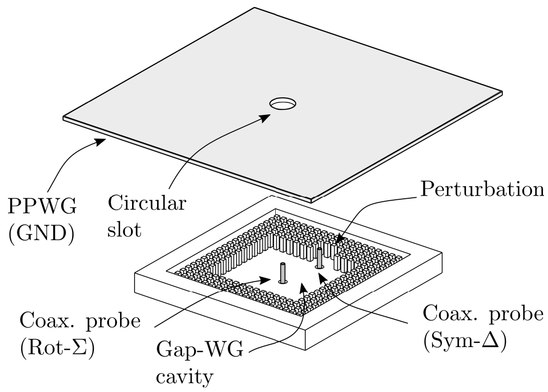

Fig. 4. Description of the cavity feed and how it is coupled to the parallel plate structure.

minimizing the unavoidable truncation involved. In the chosen geometry, the stop band that presents the bed of nails with a gap of 0.5 mm and a top metal lid goes from 18.4 to 33.3 GHz. In this frequency range the rows of pins block sufficiently the lateral propagation outwards the cavity and can replace the conventional solid wall. In this respect, it was found that three rows of pins were enough to block that unwanted propagation.

The best set of parameters found after the optimization process is indicated in Table I according to the representation depicted in Fig. 5. The penetration of the coaxial probes into the cavity was set to $h_1 = 1.70$ mm and $h_2 = 7.65$ mm for the Σ and Δ channels respectively, being their radius $R_p = 0.32$ mm.

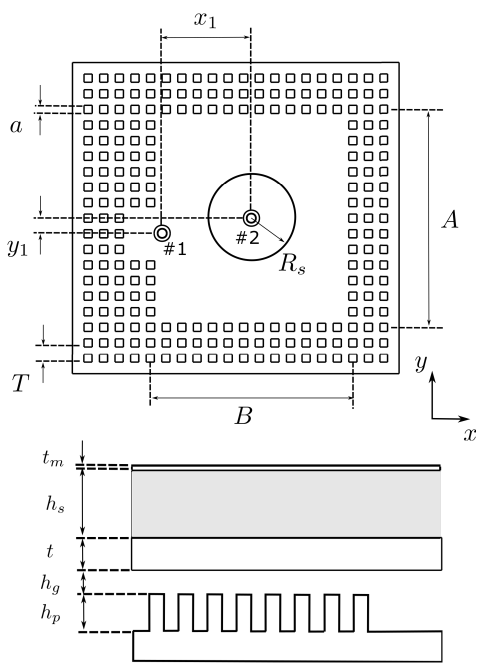

Fig. 5. Cavity feed top and side views including port numbering. Port 1 generates the Σ pattern and Port 2 generates the Δ pattern.

Fig. 6 shows the instantaneous transverse electric field distributions for the coaxial modes used to excite the PPWG, TE_{11} for the rotating field and TEM for the symmetrical one, in the ground plane at its midpoint. For the selected slot radius

TABLE I
CAVITY DIMENSIONS AS DESCRIBED IN FIG. 5

Name	Description	Value (mm)
a	Pin side	1 mm
h_p	Pin height	3.5 mm
h_g	Air gap size	0.5 mm
t	Ground plane thickness	1 mm
t_m	Metalization thickness	18 μm
T	BoN Period	1.91 mm
A	Cavity width	$14 \cdot T$
B	Cavity length	$13 \cdot T$
R_s	Slot radius	2.92 mm
x_1	Probe position	11 mm
y_1	Probe position	1.85 mm
h_s	Substrate thickness	3.175 mm

$R_s = 2.92$ mm, the TE_{11} mode is evanescent at 24 GHz but this does not have any impact on the achieved coupling given that the waveguide section is very short. Also notice that the TE_{11} in Fig. 6 (left) is maximum for $\phi = 135°$ for the chosen time instant, and that direction will rotate with time following the rotational field distribution in the cavity below.

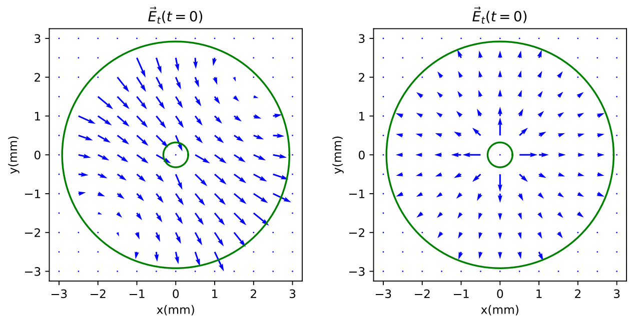

Fig. 6. Simulated instantaneous transverse electric field distributions $\vec{E}_t$ in the coaxial waveguide section (circular slot) for the rotating (left) and symmetrical (right) excitation corresponding to a TE_{11} and a TEM coaxial modes respectively.

The variation of the distributions of amplitudes and phases of E_z with the frequency within the PPWG without the slots is presented in Figs. 7 and 8. Basically, the top plots of Fig. 7 show how the amplitude distribution for the rotational phase distribution responsible for the Σ pattern is sensitive to the change with the frequency and, regarding the phase distributions, according to Fig. 8, a reasonable frequency band is expected for the Δ pattern stability, given that the perturbation method employed to generate the field distribution is intrinsically narrowband.

To gain more insight into the signal purity of the proposed solution, the amplitudes and phases of the vertical component of field E_z are shown in points angularly equispaced at a distance $R = 20$ mm from the center in Fig. 9. A linear regression line was calculated to estimate the amplitude and phase errors with respect to the ideal responses. The obtained errors are summarized in Table II. The results are worse for the phase rotating distribution but, in any case, they are acceptable for the pursued application.

To finish with the characterization of the coupling between the cavity and the homogeneous PPWG, Fig. 10 represents the simulated S-parameters corresponding to the two-port network

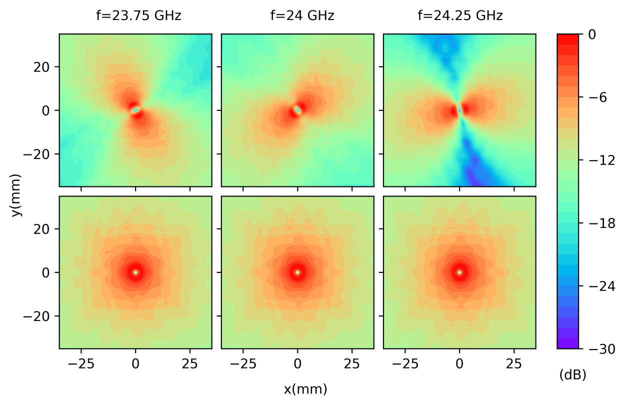

Fig. 7. Amplitude distributions (Σ above; Δ below) for the vertical electric field in the central plane of the substrate in the PPWG without slots.

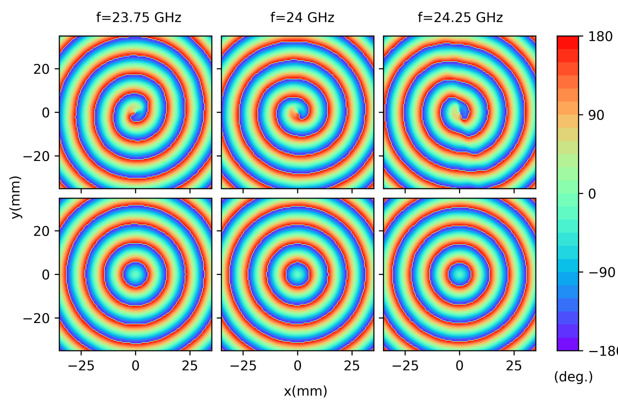

Fig. 8. Phase distributions (Σ above; Δ below) for the vertical electric field in the central plane of the substrate in the PPWG without slots.

defined by the two input ports. A good matching level and a good isolation between channels is observed at the frequency of interest.

A. Simulations of the Full RLSA Antenna

Finally, the slots were introduced in the upper layer of the parallel plate structure of Fig. 4 and simulations of the full antenna structure with the designed feed were realized. It was found that no modifications were needed in the designed cavity to keep a good response in terms of both radiation patterns and S-parameters. Fig. 11 shows the simulated radiation patterns

TABLE II
PHASE AND AMPLITUDE ERRORS FOR E_z IN THE SUBSTRATE FOR WAVEFRONTS AT $R = 20mm$

Type	Max. Phase error (deg.)	Phase std. deviation (deg.)	Max. Amplitude error (dB)
Rot.	23.5	14.7	3.3
Sym.	6.8	5.3	0.9

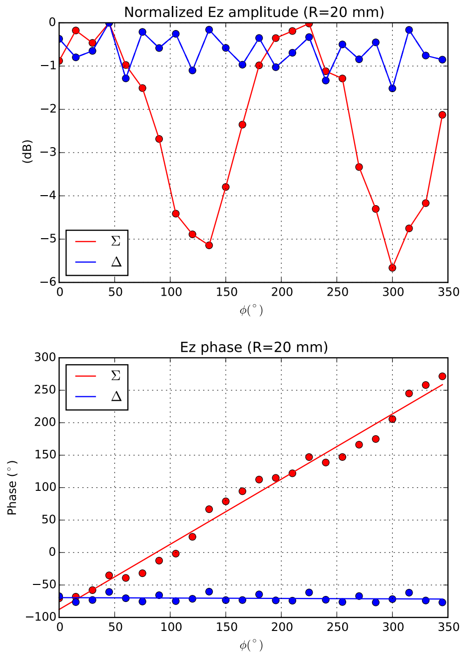

Fig. 9. Simulated amplitude and phase variations for E_z at a distance $R = 20$ mm from the center for both field distributions inside the dielectric.

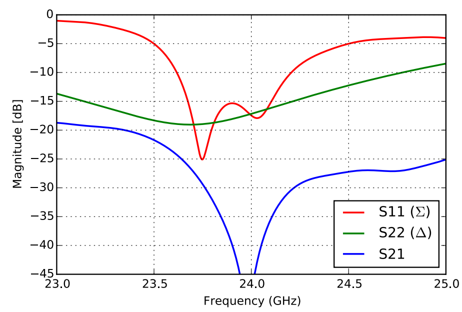

Fig. 10. Simulated S-parameters of the feed network and a PPWG without slots in Fig. 4.

obtained for different azimuth planes and for the 24 GHz frequency. A correct antenna operation is observed, although two significant sidelobes with -11 dB level appear in the planes $\phi = 0°$ and $\phi = 45°$ in the sum pattern. These sidelobes levels are 3.8 dB worse than the values showed in Fig. 3 for the MoM simulation. Regarding the other main directions, the SLL is better at the expense of a slight widen of the main lobe. This could be due to the amplitude tapering that can be observed in Figs. 7 and 9 at 24 GHz, in directions around $\phi = 135°$ and $\phi = 225°$.

The simulated S-parameters are presented in Fig. 13. At 24 GHz the isolation between channels is very good (below -40 dB) and both ports have a good impedance matching.

IV. EXPERIMENTAL RESULTS

A prototype was manufactured, assembled and measured in an anechoic chamber. Fig. 12 shows the fabricated cavity with the two coaxial probes. The cavity was manufactured by

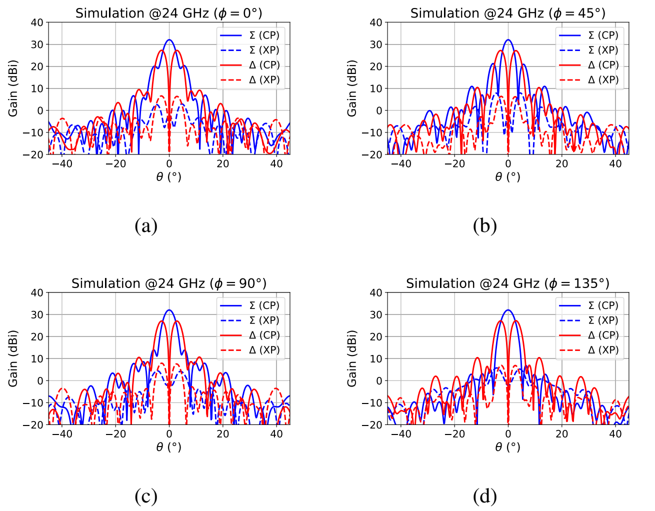

Fig. 11. Co and Crosspolar simulated radiation patterns (realized gain) for sum (Σ) and difference (Δ) channels at 24 GHz for different azimuthal angles.

conventional milling. The use of gap waveguide technology allows an easy assembling of the antenna and the feed cavity, as a good electrical contact is not required, i.e., by simple screwing them there is no risk of any leakage outside the feed cavity.

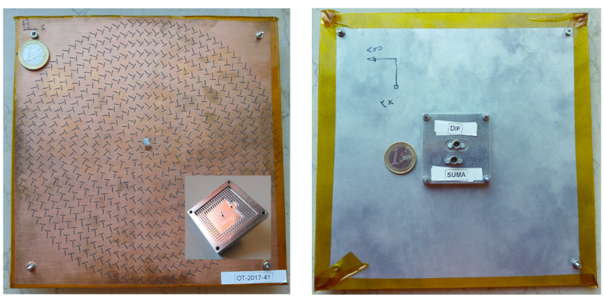

Fig. 12. Manufactured antenna and feed cavity.

Fig. 13 shows the measured S parameters together with the simulated parameters already discussed for the complete structure. There is a good agreement between simulations and measurements. It is observed that the impedance matching for both ports is below -10 dB and, although the isolation between ports deteriorates with respect to the simulations, it is still around -25 dB, which is comparable to the results obtained with other type of monopulse excitations in RLSA antennas.

The radiation patterns were also measured at the frequencies of 23.5 GHz, 24 GHz and 24.5 GHz and it was verified that there had been a frequency downshift of 0.5 GHz, with the radiation patterns at 23.5 GHz being the closest to the simulated ones presented in Fig. 11. The shift in frequencies may be due to manufacturing tolerances or inaccuracies on the estimated relative permittivity of the dielectric material. These radiation patterns at 23.5 GHz are shown in Fig. 14, where also the cross-polarization patterns are represented. Note that the cross-polarization patterns should have a minimum in the broadside direction. However, some errors in the real situation occurs. The most important one is the alignment of the cavity

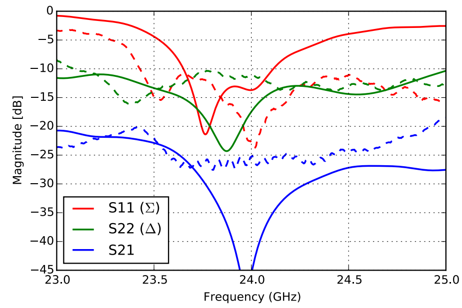

Fig. 13. Measured S-parameters (dashed lines) for the RLSA antenna. Simulated S-parameters (solid lines) are included for comparison purposes.

TABLE III
MEASURED DIRECTIVITY AND GAIN AT 23.5 GHZ

Pattern	Directivity (dBi)	Gain (dBi)
Σ	31.89	30.90
Δ	27.24	26.15

with the RLSA: small alignment errors provoke a pointing error in the co-polar of the sum pattern and an increase of the cross polar in the broadside direction. The directivity and the realized gain of the antenna are summarized in Table III. The sidelobes that appeared in the simulations in the planes $\phi = 0°$ and $\phi = 45°$ can also be observed in the measurement results.

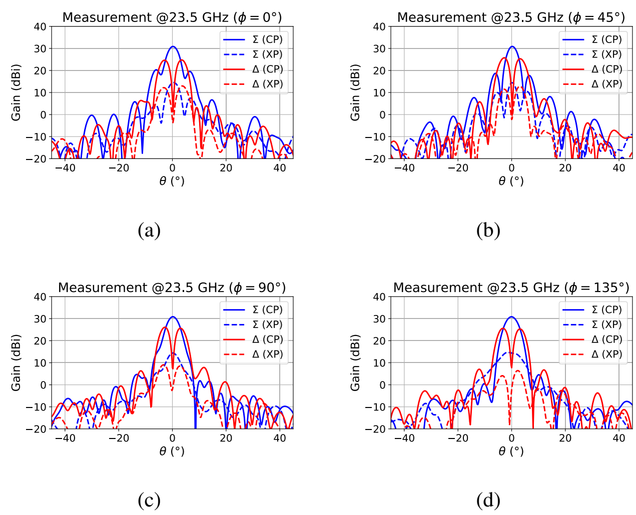

Fig. 14. Co and Crosspolar measured radiation patterns (realized gain) for Sum (Σ) and difference (Δ) channels at 23.5 GHz for different azimuthal angles.

V. CONCLUSION

The design of an antenna for a monopulse radar system is presented in this work. The antenna is a radial slot array designed with an in-house analysis and optimization software. To obtain the sum and different patterns, the antenna is fed by a cavity made in groove gap waveguide technology and excited with only two coaxial probes. The excited fields are coupled to the antenna itself by means of a circular slot in the ground plane.

A prototype working at 24 GHz with the new feed system has been designed, built and measured. The measurements confirm the correct operation of the proposed topology in terms of S-parameters, for both matching and isolation, as well as in terms of radiation patterns. The presented feed is a good alternative to other implementations based on hybrid circuits and delay lines and is especially interesting for millimeter wave frequencies, on account of its simplicity, compactness and low losses, due to the absence of dielectrics in the network responsible for the beam formation. Furthermore, the use of gap waveguide technology for the feed made the assembling of antenna and feed very simple as no electrical contact is required. The designed feed can be used as well with slots arranged in spiral configuration, then interchanging the role of the two ports. This possibility is interesting for future work since it is expected that it would provide a cleaner radiation pattern for the pencil beam. As a main drawback, the design is narrowband in nature.

VI. Acknowledgment

This work is dedicated to the memory of Professor Mariano Barba-Gea of the Technical University of Madrid (UPM), who actively helped us with the manufacturing of the prototype. He passed away unexpectedly in 2017.

References

[1] M. I. Skolnik. *Introduction to Radar Systems (2nd Edition)*. McGraw Hill Book Co., New York, 2 edition, 1980.

[2] M. Sierra Perez, J. Gismero Menoyo, M. Sierra Castañer, and A. Asensio Lopez. *Encyclopedia of RF and Microwave Engineering Chapter Monopulse Tracking Systems. Pages 3244-3255. Volume 4. (Edited by Kai Chang)*. Wiley Interscience, 2005.

[3] K. Kelly. Recent annular slot array experiments. In *1958 IRE International Convention Record*, volume 5, pages 144–152, March 1957.

[4] F. Goebels and K. Kelly. Arbitrary polarization from annular slot plannar antennas. *IRE Transactions on Antennas and Propagation*, 9(4):342–349, July 1961.

[5] M. Ando, K. Sakurai, N. Goto, K. Arimura, and Y. Ito. A radial line slot antenna for 12 GHz satellite TV reception. *IEEE Transactions on Antennas and Propagation*, 33(12):1347–1353, December 1985.

[6] M. Ando, K. Sakurai, and N. Goto. Characteristics of a radial line slot antenna for 12 GHz band satellite TV reception. *IEEE Transactions on Antennas and Propagation*, 34(10):1269–1272, October 1986.

[7] H. Sasazawa, Y. Oshima, K. Sakurai, M. Ando, and N. Goto. Slot coupling in a radial line slot antenna for 12-GHz band satellite TV reception. *IEEE Transactions on Antennas and Propagation*, 36(9):1221–1226, Sep 1988.

[8] J. Takada, A. Tanisho, K. Ito, and M. Ando. Circularly polarised conical beam radial line slot antenna. *Electronics Letters*, 30(21):1729–1730, Oct 1994.

[9] A. Akiyama, T. Yamamoto, M. Ando, and E. Takeda. Conical beam radial line slot antennas for 60 GHz band wireless LAN. In *IEEE Antennas and Propagation Society International Symposium. 1998 Digest. Antennas: Gateways to the Global Network. Held in conjunction with: USNC/URSI National Radio Science Meeting (Cat. No.98CH36*, volume 3, pages 1421–1424 vol.3, June 1998.

[10] S. Hosono, J. Hirokawa, M. Ando, N. Goto, and H. Arai. A rotating mode radial line slot antenna fed by a cavity resonator. In *Proceedings of IEEE Antennas and Propagation Society International Symposium and URSI National Radio Science Meeting*, volume 3, pages 2200–2203 vol.3, June 1994.

[11] M. Sierra P, J. M. Salamanca, M. V. Isasa, and M. S. Castañer. Synthesis of circularly polarised multiprobe feed radial line slot array. In *IEEE Antennas and Propagation Society International Symposium. 1998 Digest. Antennas: Gateways to the Global Network. Held in conjunction with: USNC/URSI National Radio Science Meeting (Cat. No.98CH36)*, volume 2, pages 1184–1187 vol.2, June 1998.

[12] M. Albani, A. Mazzinghi, and A. Freni. Automatic design of CP-RLSA antennas. *IEEE Transactions on Antennas and Propagation*, 60(12):5538–5547, Dec 2012.

[13] M. Sierra-Castañer, M. Sierra-Perez, M. Vera-Isasa, and J. L. Fernandez-Jambrina. Low-cost monopulse radial line slot antenna. *IEEE Transactions on Antennas and Propagation*, 51(2):256–263, Feb 2003.

[14] Lizhi You and W B. Dou. A compact monopulse radial line slot array antenna at millimeter wavelengths. *International Journal of Infrared and Millimeter Waves*, 28:811–820, 10 2007.

[15] A. Vosoogh, A. Haddadi, A. U. Zaman, J. Yang, H. Zirath, and A. A. Kishk. w-band low-profile monopulse slot array antenna based on gap waveguide corporate-feed network. *IEEE Transactions on Antennas and Propagation*, 66(12):6997–7009, Dec 2018.

[16] A. Tamayo-Dominguez, J. Fernandez-Gonzalez, and M. S. Castaner. Low-cost millimeter-wave antenna with simultaneous sum and difference patterns for 5g point-to-point communications. *IEEE Communications Magazine*, 56(7):28–34, July 2018.

[17] M. S. Castañer, J. I. G. Fuertes, J. M. S. G. de Olea, R. M. Gallego, and J. L. F. Jambrina. Radial line slot antenna design for monopulse space debris radar. In *2016 10th European Conference on Antennas and Propagation (EuCAP)*, pages 1–4, April 2016.

[18] M. Sierra-Castañer, A. Tamayo Dominguez, M. Barba Gea, E. Rajo-Iglesias, and J.L. Vazquez-Roy. Monopulse RLSA Antenna at 24 GHz Based on a Gap-Waveguide Cavity Feed. In *2017 European Microwave Conference (Nuremberg, Germany)*, Oct. 2017.

[19] E. Rajo-Iglesias and P. S. Kildal. Groove gap waveguide: A rectangular waveguide between contactless metal plates enabled by parallel-plate cut-off. In *Proceedings of the Fourth European Conference on Antennas and Propagation*, pages 1–4, April 2010.

[20] P.-S Kildal, E. Alfonso, A. Valero-Nogueira, and E. Rajo-Iglesias. Local metamaterial-based waveguides in gaps between parallel metal plates. *IEEE Antennas and Wireless Propagation Letters*, 8:84–87, 2009.

[21] P.-S. Kildal, A.U. Zaman, E. Rajo-Iglesias, E. Alfonso, and A. Valero-Nogueira. Design and experimental verification of ridge gap waveguide in bed of nails for parallel-plate mode suppression. *IET Microwaves, Antennas, Propag.*, 5(3):262 –270, 21 2011.

[22] T. Salmeron-Ruiz, T. Diez-Ricondo, and M. Sierra-Castañer. An optimization procedure for radial line slot antennas with arbitrary pattern. In *The 8th European Conference on Antennas and Propagation (EuCAP 2014)*, pages 1793–1796, April 2014.

[23] T. Nguyen, R. Jayawardene, K. Sakurai, J. Hirokawa, M. Ando, M. Sierra-Castañer, O. Amano, S. Koreeda, T. Matsuzaki, and Y. Kamata. Propagation characteristics of honeycomb structures used in mm-wave radial line slot antennas. *IEICE Transactions*, 97-B(6):1139–1147, 2014.

[24] T. Nguyen, J. Hirokawa, M. Ando, and M. Sierra-Castañer. Design of mm-Wave RLSA with lossy waveguides by slot coupling control techniques. *IEICE Transactions on Communications*, E98-B(9):1865–1872, Sep. 2015.

[25] M. Sierra-Castañer, M. Sierra-Perez, M. Vera-Isasa, and J. L. Fernandez-Jambrina. Fast analysis model for radial-line slot antennas. *Microwave and Optical Technology Letters*, 44(1):17–21, 2005.

Jose Luis Vazquez-Roy (M'00) was born in Madrid, Spain, in 1969. He received the Ingeniero de Telecomunicación and Ph.D. degrees from the Universidad Politécnica de Madrid, Madrid, Spain, in 1993 and 1999, respectively. In 1999, he joined the Teoria de la Señal y Comunicaciones Department, Universidad Carlos III de Madrid, Spain, where he is currently an Associate Professor. His research activities and interests include the analysis and design of planar antennas, gap-waveguide technology, and the development of millimeter-wave components for communication and radar systems.

Adrián Tamayo Domínguez was born in Madrid, Spain, in 1991. He received the M.Sc degree in Telecommunication Engineering from Universidad Politécnica de Madrid in 2016. He is Ph.D. student at Universidad Politécnica de Madrid thanks to a grant for PhD studies from Spanish Ministry of Education and Science since 2015. He visited the KTH Royal School of Technology, Stockholm, Sweden, during a doctoral stay in 2017. He was the recipient of the Young Researchers Award at URSI 2018 in Granada, Spain, and finalist of the Student Paper Competition at GSMM 2018 in Boulder, Colorado. His current research interest is RF circuits, gap waveguides and higher symmetries applied to planar antenna applications oriented to 5G developing.

Eva Rajo-Iglesias was born in Monforte de Lemos, Spain, in 1972. She received the M.Sc. degree in telecommunication engineering from the University of Vigo, Spain, in 1996, and the Ph.D. degree in telecommunication engineering from the University Carlos III of Madrid, Spain, in 2002.

She was a Teacher Assistant with the University Carlos III of Madrid from 1997 to 2001. She joined the Polytechnic University of Cartagena, Cartagena, Spain, as a Teacher Assistant, in 2001. She joined University Carlos III of Madrid as a Visiting Lecturer in 2002, where she has been an Associate Professor with the Department of Signal Theory and Communications since 2004. Since 2018 she is Full Professor in the same department. She visited the Chalmers University of Technology, Göteborg, Sweden, as a Guest Researcher, in 2004, 2005, 2006, 2007, and 2008, and has been an Affiliate Professor with the Antenna Group, Signals and Systems Department, since 2009 to 2016. She has co-authored more than 70 papers in JCR international journals and more than 100 papers in international conferences. Her current research interests include microstrip patch antennas and arrays, metamaterials, artificial surfaces and periodic structures, gap waveguide technology, MIMO systems and optimization methods applied to electromagnetism.

Dr. Rajo-Iglesias was the recipient of the Loughborough Antennas and Propagation Conference Best Paper Award in 2007, the Best Poster Award in the field of Metamaterial Applications in Antennas, at the conference Metamaterials 2009, the 2014 Excellence Award to Young Research Staff at the University Carlos III of Madrid and the Third Place Winner of the Bell Labs Prize 2014. She is currently an Associate Editor of the IEEE ANTENNAS AND PROPAGATION MAGAZINE and has served as Associate Editor of the IEEE ANTENNAS AND WIRELESS PROPAGATION LETTERS (2011-2017).

Manuel Sierra Castañer (IEEE SM) was born in 1970 in Zaragoza (Spain). He obtained the degree of Telecommunication Engineering in 1994 and the PhD in 2000, both from the Technical University of Madrid (UPM) in Spain. He worked for the cellular company Airtel from 1995 to 1997. Since 1997, he worked in the University ”Alfonso X” as assistant, and since 1998 at Technical University of Madrid as research assistant, assistant, associate professor, and finally Full Professor since 2017. He has been visitor researcher in Tokyo Tech (September-December 1998) and EPFL (September-December 1999) during his PhD and visitor Professor in Tokyo Tech during the summers of 2012 and 2013. Currently, he is Senior member of the IEEE and AMTA Societies. His current research interests are in planar antennas and antenna measurement systems. Dr. Sierra-Castañer obtained the IEEE APS 2007 Schelkunoff Prize paper Award for the paper “Dual-Polarization Dual-Coverage Reflectarray for Space Applications” in 2007 and other awards for papers in conferences. Since January 2015 he is the AMTA Europe liaison, and since January 2016 he is member of the EurAAP board of directors, where he is currently the vice-chair.